32nd Congress of the International Council of the Aeronautical Sciences
September 6-10, 2021
Pudong Shangri-La, Shanghai, China

Applied Research on Supervised Learning in the Judgment of Airfoil Transition

Binbin Wei, Yongwei Gao, Dong Li

School of Aeronautics Northwestern Polytechnical University

Abstract: This paper combines the latest machine learning techniques to develop an effective and reliable supervised learning model for transition judgment. Firstly, the variable-interval time average (VITA) method is used to transform the fluctuating pressure signal into a sequence of states in the Markov state space. Then we describe it using Markov chain model, and obtain its feature vectors. Then the hidden Markov model is used to pre-classify the feature vectors labeled using the traditional RMS criteria. And finally a classification model based on probability density distribution is established. The research shows that the model developed in this paper is effective and reliable and possesses a generalization ability. Compared with the traditional RMS criterion, a reasonable 'transition zone' can be obtained using the developed classification model without comparing the signals at multiple locations.

Keywords: supervised learning, transition judgment, classification model, Markov chain model, hidden Markov model

1 Introduction

Judging the transition has always been a frontier issue in the field of aerodynamics. It is hoped to develop an effective and reliable supervised learning model for the judgment or prediction on transition in this paper.

Presently, most of the research on transition is still based on experimental method. The commonly used transition detection methods in experiment are hot wire method[1],[2], temperature sensitive paints method[3], infrared thermography[4], hot-film techniques[5] and flow visualization methods[6] and so on. These methods have their own defects. Hot wire anemometry is intrusive and provides only point-wise flow information. Temperature sensitive paints should coat the model before experiment. Infrared thermography and hot film sensors seem too complicated. But above all, these techniques are not convenient for flight test or practical flow control. Therefore, it is still necessary to seek convenient, effective and practical transition detection method for unsteady aerodynamics.

Compared with the above experimental techniques, it is more convenient and practical for pressure transducers to detect boundary layer characteristics. Early in 1970s, Helle[7] using acoustic technique detected flow transition on hypersonic re-entry vehicles. Lews and Banner[8] using surface pressure fluctuation measurements investigated the boundary layer transition on the X-15 vertical fin. With the progress of technology of pressure transducer manufacture, the transducer rapid response and miniaturization have been improved greatly. The pressure transducer measurement technique for steady flow transition detection has now applied to wide velocity range from low-speed flow to hypersonic in wind tunnel experiment.

In this paper, a supervised learning model for transition judgment is established by using fluctuating pressure signals on airfoil surface. It is hoped that the model can calculate the transition zone to a certain extent rather than a ‘transition point’ obtained by traditional transition criterion.

Firstly, the variable-interval time average (VITA) method[10]-[12] is used to convert the fluctuating pressure signal on the airfoil surface into the state sequence in Markov state space. Then, the Markov chain model is used to describe it, and the feature vectors are obtained. Then the hidden Markov model[13]-[16] is used to pre-classify the feature vectors labeled using the traditional root mean square (RMS) criteria. Finally, a classification model based on probability density distribution is established.

The results show that the classification model developed in this paper is reliable and effective. The experimental data of different Reynolds numbers can be reliably predicted by using the same Reynolds number experimental data for model training. Compared with the traditional RMS criterion, a reasonable ‘transition zone’ can be obtained using the developed model and it does not require signals from multiple locations for comparison.

2 Mathematical method

The mathematical methods used in this paper which are VITA method, Markov chain model and Hidden Markov model are introduced in this section.

2.1 Variable-Interval Time Average method[10]

In the time series of fluctuating pressure, the VITA variance of fluctuating pressure is defined as:

$$Var(t,T)=\frac{1}{T}\int_{t-\frac{T}{2}}^{t+\frac{T}{2}}p^2(\tau)d\tau-[\frac{1}{T}\int_{t-\frac{T}{2}}^{t+\frac{T}{2}}p(\tau)d\tau]^2 \tag{1}$$

where T is the average time interval.

When $T\to\infty$, the second item of the right side of Equ. 1 is 0 and the Var (t,T) is equal to the mean-square value in general sense. So the VITA method essentially plays the role of low-pass filtering.

The detection function is defined as:

$$D(t)=\begin{cases}1 & Var(t,T)\geq KP_{rms}^2\\ 0 & otherwise\end{cases} \tag{2}$$

where K is the threshold and P_{rms} is the RMS value.

The fluctuating pressure time sequence can be finally converted into a state sequence D using the VITA method which can be regarded as a Markov state space.

2.2 Markov chain model

The Markov chain model is a random sequence model which corresponds to a state of a system.

Considering the random process $\left\{X^{(n)},n=0,1,2,\cdots\right\}$, which takes a value of a valid or countable set M, the state space is assumed to be $M=\left\{0,1,2,\cdots\right\}$, and the elements in M are called the state of the random process.

Definition 1 Assuming that there is a fixed probability P_{ij} independent of time, making

$$P(X^{(n+1)}=i\,|\,X^{(n)}=j,X^{(n-1)}=i_{n-1},\cdots,X^{(0)}=i_0)=P_{ij},\quad n\geq 0 \tag{3}$$

where $i,j,i_0,i_1,\cdots,i_{n-1}\in M$, the random process is called a Markov chain.

The probability P_{ij} represents the probability of transitioning from a given current state j to state i, obviously with

$$P_{ij}\geq 0,\quad \sum_{i=0}^{\infty}P_{ij}=1,\ \ j=0,1,\cdots \tag{4}$$

Definition 2 A matrix consisting of transition probability matrices

$$P=\begin{bmatrix} P_{00} & P_{01} & \cdots \\ P_{10} & P_{11} & \cdots \\ \vdots & \vdots & \vdots \end{bmatrix}$$

is called a one-step transition probability matrix. And P^n is called a *n*-step transition probability matrix.

Definition 3 The vector $\vec{\pi}=(\pi_0, \pi_1, \cdots, \pi_{k-1})^T$ is called the stationary distribution of a finite Markov chain if it satisfies

$$\begin{aligned} &\pi_i \geq 0, \quad \sum_{i=0}^{k-1}\pi_i = 1 \\ &P\vec{\pi}=\vec{\pi} \end{aligned} \tag{5}$$

That is $\sum_{j=0}^{k-1} P_{ij}\pi_j=\pi_i$, $\lim_{n\to\infty}\left\|X^{(n)}-\vec{\pi}\right\|=\lim_{n\to\infty}\left\|P^n X^{(0)}-\vec{\pi}\right\|=0$, where $\|\bullet\|$ represents the norm of the vector.

2.3 Hidden Markov model

There are two states in the hidden Markov model: the observable state and hidden state. Let's have *m* hidden states and *n* observable states. The stationary distribution of these hidden states is assumed to be $\vec{\alpha}=(\alpha_1, \alpha_2, \cdots, \alpha_m)$. And the stationary distribution of the observable states is $(p_{k1}, p_{k2}, \cdots, p_{kn})$ when the hidden state is k ($k=1,2,\cdots,m$).

The stationary distribution of the hidden states and the observable states satisfies the formula as follows.

$$\sum_{k=1}^{m}\alpha_k = 1, \sum_{i=1}^{n} p_{ki} = 1 \tag{6}$$

In the case of ignoring the hidden state, the observable state obeys the following single-step transition probability matrix.

$$P_2=\begin{bmatrix} p_{00} & p_{01} & \cdots & p_{m1} \\ p_{10} & p_{11} & \cdots & p_{m2} \\ \vdots & \vdots & \vdots & \vdots \\ p_{1n} & p_{2n} & \cdots & p_{mn} \end{bmatrix}\begin{bmatrix} \alpha_1 & \alpha_1 & \cdots & \alpha_1 \\ \alpha_2 & \alpha_2 & \cdots & \alpha_2 \\ \vdots & \vdots & \vdots & \vdots \\ \alpha_m & \alpha_m & \cdots & \alpha_m \end{bmatrix}=\vec{p}(1,1,\cdots,1) \tag{7}$$

where $\vec{p}=(\sum_{k=1}^{m}\alpha_k p_{k1}, \sum_{k=1}^{m}\alpha_k p_{k2}, \cdots, \sum_{k=1}^{m}\alpha_k p_{kn})^T$. It is easy to verify that the vector $\vec{p}$ is a stationary distribution of P_2.

If a distribution $\vec{q}$ is observed, the transition probability of the hidden state can be obtained by solving the following problem.

$$\begin{aligned} &\min_{\alpha}\left\|\vec{p}-\vec{q}\right\|_2^2 \\ &s.t. \quad \sum_{k=1}^{m}\alpha_k = 1, \ \alpha_k \geq 0 \end{aligned} \tag{8}$$

This problem is a constrained minimum quadratic problem whose solution method is very mature. The SUMT outer point penalty method was used in this paper.

3 Establishment of a supervised learning model

The airfoil wind tunnel experiment was carried out in the NF-3 wind tunnel. The experimental model chord length was *c*=600mm and the experimental Reynolds number was $\mathrm{Re}=0.8\times10^6$, $\mathrm{Re}=1.1\times10^6$ and

$\mathrm{Re}=2.0\times10^{6}$.

3.1 Establishment of state space

The VITA method is used to convert the fluctuating pressure of the airfoil into a state in the state space. The fluctuating pressure data in the case of $\mathrm{Re}=1.1\times10^{6}$, $\alpha=2°$ is taking as an example.

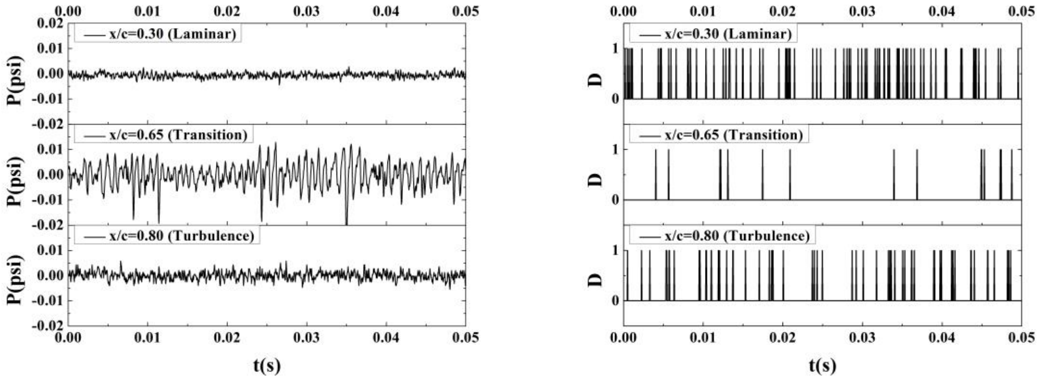

(a) Fluctuating pressure waveform (b) Detection function of the VITA method

Fig.1 Fluctuating feature and detection function at the typical location of $\alpha=2°$

The fluctuating pressure and its corresponding detection function calculated by the VITA method are shown in Fig.1 and the parameters of the threshold *K* and *T* was set to *K*=1.0 and *T*=0.00025s. It can be seen that the detection function of the transition position is significantly different from the laminar and turbulence flow that the detection function of the transition zone is mostly *D*=0.

The number of data whose detection function is *D*=1 in Fig.1 is calculated, and the cumulative time Δt is calculated as shown in Fig.2.

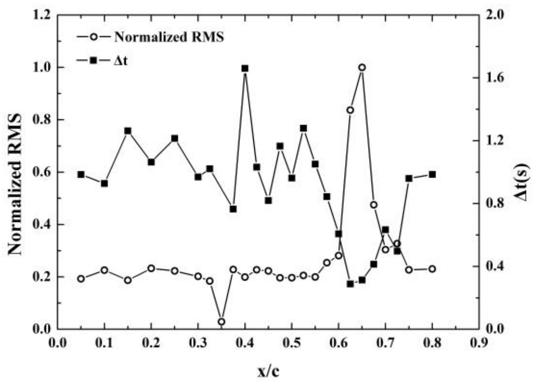

Fig.2 Comparison of the RMS and VITA result

The comparison of the fluctuating pressure RMS value with the cumulative time Δt calculated by the VITA method in the case of $\mathrm{Re}=1.1\times10^{6}$ is shown in Fig.2 where the open circle is the dimensionless RMS result and the solid square is the cumulative time. It can be seen that the minimum cumulative time position corresponds to the RMS peak position.

3.2 Establishment of Markov chain model

The state space calculated using the VITA method (*K*=1.0, *T*=0.00025s) at x/c=0.65 position (transition) in Fig.1 was analyzed.

Its transition probability matrix is:

$$P = \begin{bmatrix} 0.927 & 0.805 \\ 0.073 & 0.195 \end{bmatrix}$$

Its steady state probability distribution can be calculated by P^n and it is $\vec{\pi} = [0.917 \quad 0.083]^T$. So the Markov chain model of the data at this location is

$$\begin{cases} X^{(n+1)} = P \cdot X^{(n)} \\ X^{(n+1)} = P^{n+1} \cdot X^{(0)} = \vec{\pi} \cdot E \cdot X^{(0)} \end{cases} \tag{19}$$

The model is uniquely identified by the transition probability matrix P and its steady-state probability distribution $\vec{\pi}$, so the data can be characterized by P and $\vec{\pi}$. A vector composed of components of P and $\vec{\pi}$ was used as a feature vector of the signal, namely $\vec{v} = \left[P_{00}, P_{10}, P_{01}, P_{11}, \vec{\pi_1}, \vec{\pi_2}\right]^T$. After normalization, the feature vector is $\vec{V} = [0.309, 0.024, 0.268, 0.065, 0.306, 0.028]^T$.

The feature attributes of all hidden attributes (transition and non-transition) in the sampled data were averaged and were used as a stationary distribution of the observable state in the hidden Markov model.

3.3 Solution of hidden Markov model

The experimental data in the case of $\mathrm{Re} = 1.1 \times 10^6$ is used to solve the hidden Markov model. The parameter is selected as K=1.0, T=0.00025s.

After solving the least quadratic problem, the smooth distribution of hidden attributes is obtained as shown in Fig.3(a). Since there are only two hidden attributes, the distribution can also be described as shown in Fig.3(b).

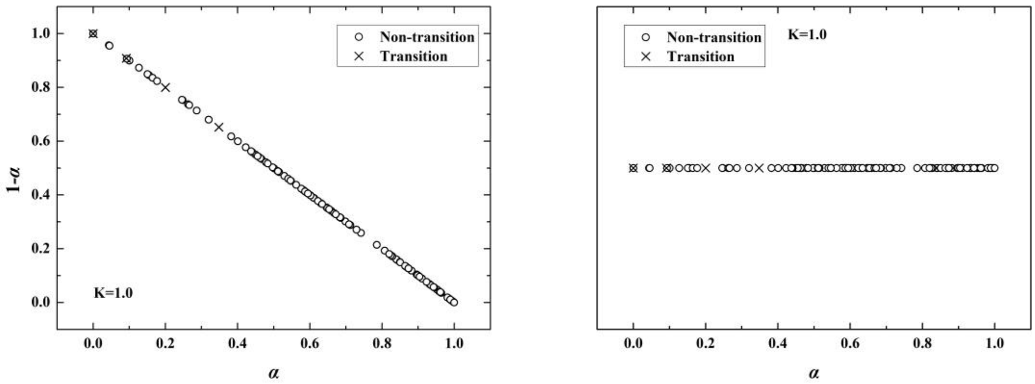

(a) 2-D distribution (b) 1-D distribution

Fig.3 Distribution of the hidden state

As can be seen from Fig.3, the distribution of the two hidden attributes (transition and non-transition) overlaps in some areas, which results in unclear classification boundaries. And we proposed a classification model based on probability density distribution in order to improve this situation.

3.4 Establishment and verification of classification model

Considering the distribution of Fig.3, we consider that the two hidden attributes are subject to different probability density distributions. Let's assumed that it follows a Gaussian distribution within the interval [0,1], and the probability outside the interval is zero, which is

$$y=\begin{cases}0 & \alpha<0\\ c\cdot e^{-\frac{(\alpha-\mu)^2}{2\sigma^2}} & 0\le\alpha\le 1.0\\ 0 & \alpha>1.0\end{cases} \tag{2}$$

where μ is the mean value, σ is the standard deviation, and c is a constant satisfying $\int_{-\infty}^{\infty} y d\alpha = 1$, that is

$$c = 1 \Big/ \int_{\alpha=0}^{\alpha=1.0} e^{-\frac{(\alpha-\mu)^2}{2\sigma^2}} d\alpha \tag{3}$$

The probability density distributions of two hidden attributes are shown in Fig.4, and the solid line is the probability density distribution of the transition, and the dotted line is the non-transition probability density distribution.

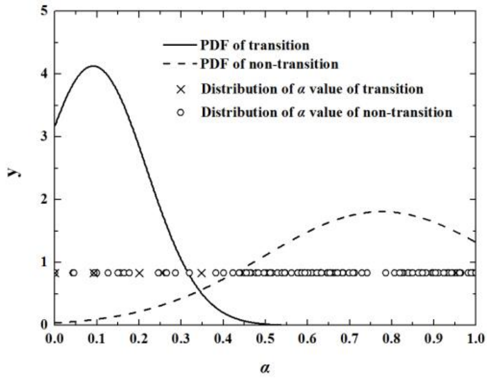

Fig.4 Probability density distribution

Let the α value of a signal be α_0 and its distance from the mean value of the distance probability density distribution is $\Delta = |\mu - \alpha_0|$ and calculate its confidence $1-\beta$.

$$1-\beta = \int_{\alpha=\mu-\Delta}^{\alpha=\mu+\Delta} y d\alpha \tag{12}$$

The β value of transition and non-transition could be calculated through Equ. (12) in the case of $\alpha = \alpha_0$. And we can calculate the probability of transition or non-transition through the following formula.

$$p_1 = \frac{\beta_1}{\beta_1+\beta_2},\ \ p_2 = \frac{\beta_2}{\beta_1+\beta_2} \tag{13}$$

where β_1 is the β value of transition, β_2 is the β value of non-transition, p_1 is the probability of transition, p_2 is the probability of non-transition.

4 Analysis and discussions

The experimental data with the Reynolds number of $\mathrm{Re} = 1.1\times10^6$ at $\alpha = 0° \sim 7°$ are used to train the model in this section. The prediction results of $\mathrm{Re} = 1.1\times10^6$ are shown, and the results of generalization of the model to other Reynolds numbers are discussed.

4.1 Prediction results of training data

Model training and prediction are performed using experimental data of $\mathrm{Re}=1.1\times10^{6}$, and the model parameters are selected as *K*=1.0, *T*=0.00025s.

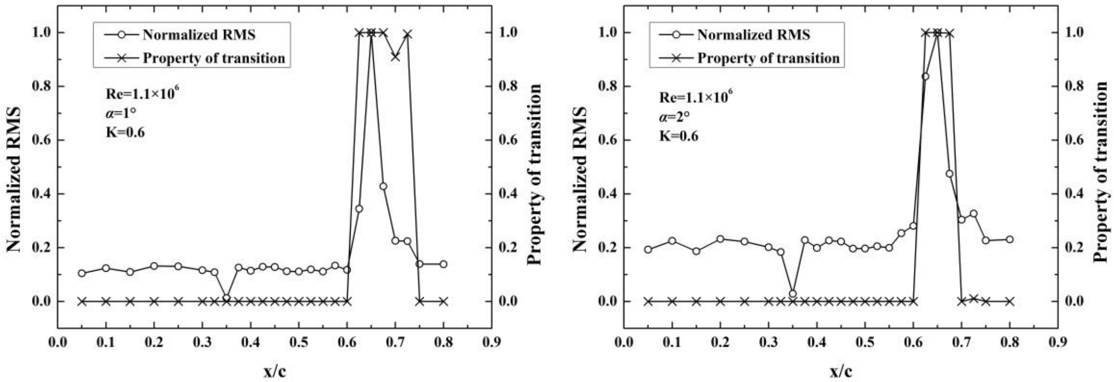

(a) $\alpha=1°$ (b) $\alpha=2°$

Fig.5 Prediction results of the training data itself ($\mathrm{Re}=1.1\times10^{6}$)

Fig.5 is a prediction result of the training data itself ($\mathrm{Re}=1.1\times10^{6}$), where (a) is a case of $\alpha=1°$, and (b) is a case of $\alpha=2°$. The open circle is a normalized RMS result, and the cross is the predicted result of the developed model. A ‘transition point’ can be only judged using the traditional RMS criterion, while a reasonable ‘transition zone’ can the obtained using the developed method. And the ‘transition point’ judged by the traditional criterion is located in the ‘transition zone’. To some extent, the reliability of the two methods is demonstrated.

In this paper, the traditional RMS criterion is used to label the data. In Fig.5, only one transition position can be labeled for each angle of attack. It is worth noting that when using the developed model for prediction, it is possible to predict multiple transition positions at one angle of attack.

4.2 Generalization results of other Reynolds numbers

The model trained in Section 4.1 is generalized to the case of $\mathrm{Re}=0.8\times10^{6}$ and $\mathrm{Re}=2.0\times10^{6}$ in this section.

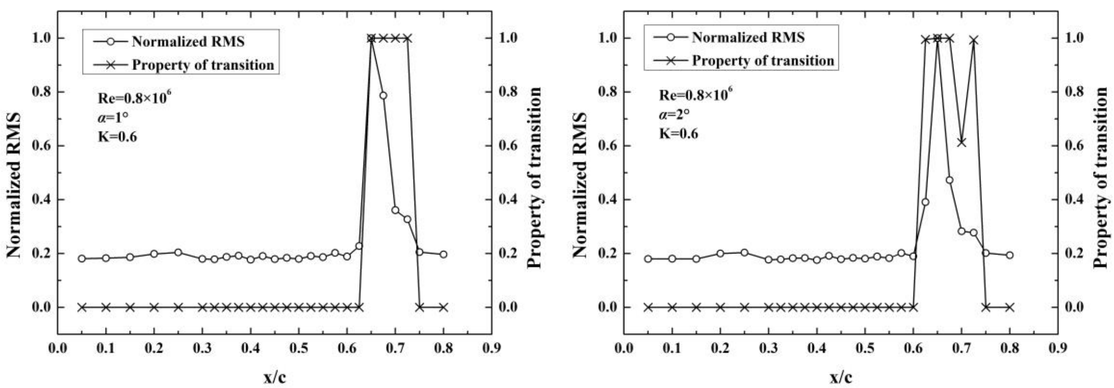

(a) $\alpha=1°$ (b) $\alpha=2°$

Fig.6 Generalization result of $\mathrm{Re}=0.8\times10^{6}$

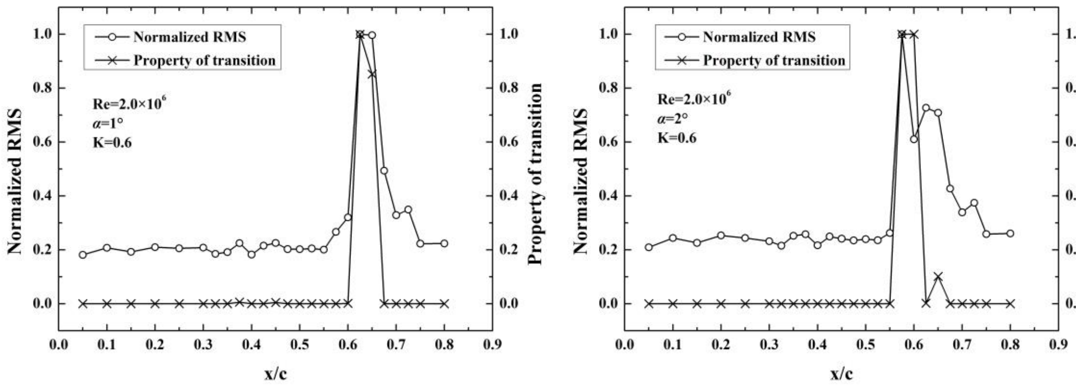

(a) $\alpha = 1°$ (b) $\alpha = 2°$

Fig.7 Generalization result of $\mathrm{Re} = 2.0 \times 10^6$

Fig.6 and Fig.7 are the generalization results for $\mathrm{Re} = 0.8 \times 10^6$ and $\mathrm{Re} = 2.0 \times 10^6$ respectively, where (a) is the case of $\alpha = 1°$, and (b) is the case of $\alpha = 2°$. The open circle is a dimensionless RMS result, and the cross is the predicted result of the model. Same as in Fig.5, a ‘transition point’ can be only judged using the traditional RMS criterion, while a reasonable ‘transition zone’ can the obtained using the developed method..

It can be seen from Fig.5 to Fig.7 that, using the experimental data of the same Reynolds number for model training, we can predict the transition results under different Reynolds numbers, which indicates that the classification model developed in this paper possesses strong generalization ability. Compared with the traditional RMS criterion, a reasonable ‘transition zone’ correspond to the ‘transition point’ determined by the RMS criterion can be obtained using the developed prediction model, indicating that the classification model developed in this paper is reliable and effective.

5 Conclusions

In this paper, the VITA method is used to transform the fluctuating pressure signal into a state sequence in the Markov state space. Then, it is described by Markov chain model, and its feature vector is obtained. Then the hidden Markov model is used to pre-classify the feature vectors labeled using the traditional RMS criteria, and finally a classification model based on probability density distribution is established. The model is trained using the experimental data in the case of same Reynolds number, and it is generalized to different Reynolds numbers, and the results show that the developed model possesses strong generalization ability. Compared with the traditional RMS criterion, a reasonable ‘transition zone’ can be obtained using the developed classification model and it does not require signals from multiple locations for comparison.

Acknowledgement

Thanks to all the experimental staff of NF-3 wind tunnel for their hard work.

Copyright Statement

paper, for the publication and distribution of this paper as part of the ICAS proceedings or as individual off-prints from the proceedings.

References

[1] Knapp CF, Roache PJ (1968) A combined visual and hot-wire anemometer investigation of boundary-layer transition. AIAA Journal 6:29-36 DOI 10.2514/3.4437

[2] Lagraff JE (1972) Observations of Hypersonic Boundary-Layer Transition Using Hot Wire Anemometry. AIAA Journal 10:762-769 DOI 10.2514/3.50208

[3] Costantini M, Fey U, Henne U, Klein C (2015) Nonadiabatic Surface Effects on Transition Measurements Using Temperature-Sensitive Paints. AIAA Journal 53:1172-1187 DOI 10.2514/1.J053155

[4] Giepman RHM, Schrijer FFJ, van Oudheusden BW (2015) Infrared Thermography Measurements on a Moving Boundary-Layer Transition Front in Supersonic Flow. AIAA Journal:1-5 DOI 10.2514/1.J053910

[5] Richter K, Koch S, Gardner A, Mai H, Klein A, Rohardt C (2014) Experimental Investigation of Unsteady Transition on a Pitching Rotor Blade Airfoil. Journal of the American Helicopter Society 59:1-12

[6] Schülein E, Rosemann H, Schaber S (2012) Transition detection and skin friction measurements on rotating propeller blades. Paper AIAA-2012-3202, 28th AIAA aerodynamic measurement technology, ground testing and flight testing conference, New Orleans, Louisiana, 25–28 June 2012. doi: 10.2514/6.2012-3202

[7] Heller HH (1969) Acoustic technique for detection of flow transition on hypersonic re-entry vehicles. AIAA Journal 7:2227-2232 DOI 10.2514/3.5520

[8] Lewis TL, Banner RD (1971) Boundary layer transition detection on the X-15 vertical fin using surface-pressure-fluctuation measurements. NASA TM X-2466

[9] Gao Y, Zhu Q, Wang L. Measurement of unsteady transition on a pitching airfoil using dynamic pressure sensors[J]. Journal of Mechanical Science & Technology, 2016, 30(10):4571-4578.

[10] R. F. Blackwelder, R. E. Kaplan. On the Wall Structure of the Turbulent Boundary Layer[J]. Journal of Fluid Mechanics, 1976, 76(1):89-112.

[11] Ferrier M , Chokani N . Hypersonic Transition Detection with Single Point Hot-Wire Measurements[C]// Aerospace Sciences Meeting & Exhibit. 2003.

[12] Chokani N . VITA measurements of transition in transitional hypersonic boundary layer flows[J]. Experiments in Fluids, 2005, 38(4):440-448.

[13] Ching W K , Ng M K . Building simple hidden Markov models.[J]. International Journal of Mathematical Education in Science & Technology, 2004, 35(2):296-299.

[14] Koski T . Hidden Markov models for bioinformatics[J]. Journal of the Royal Statistical Society, 2001, 167(1):194-195.

[15] Rabiner L R . A Tutorial on Hidden Markov Models and Selected Applications in Speech Recognition[J]. proc.IEEE, 1989, 77.

[16] Pederson S P . Hidden Markov and Other Models for Discrete valued Time Series[J]. International Journal of Forecasting, 1997, 40(3):263-263.